

Content

Introduction	2
Key parameters for FSOC	3
Cloud cover	3
Turbulence	4
Fried parameter r_0	4
Isoplanatic angle θ_0	4
Coherence time τ_0	4
Scintillation	5
Refractive index structure parameter C_n^2	6
Aerosols	6
Water vapor	7
Overview of the instrumental solutions of Miratlas	7
The Sky Monitor	8
Weather parameters	8
Turbulence	9
Daytime measurement using solar scintillation	9
Daytime measurement with SHABAR (optional)	10
Nighttime measurement with C-DIMM	12
Irradiance	13
Irradiance measurement	13
Radiance measurement (optional)	13
Thermal infrared irradiance	14
Aerosols	14
Differential absorption solar photometer (optional)	14
Precipitable water vapor	14
Allsky cameras	15
Visible allsky cameras	15
LWIR thermal allsky cameras (optional)	17

Introduction

Miratlas offers instruments for a complete characterization of the atmosphere. Our solutions have been developed for free-space optical communication (FSOC) and carrier grade applications, including satellite data offload, feeder links, GEO constellations and quantum communications.

Direct to Earth laser communication (Laser Comms) is a groundbreaking technology for transmitting data from the ground to a satellite using optical signals sent through the atmosphere. It offers decisive advantages over classical radiofrequency (RF) communications.

- **Higher bandwidth:** FSOC provides higher bandwidth than RF. It enables faster transmission of data, video, and voice, as well as lower latency for time critical usages such as high-speed trading.
- **Secure communication:** FSOC is less susceptible to interception and jamming than RF. Narrow optical beams are difficult to intercept without being in the line-of-sight.
- **Quantum communication capable:** optical links are the only way to exchange entangled photons over long distances.
- **Low interference:** Narrow optical beams are unlikely to interfere with other light sources such as the atmosphere, other satellites, or ground-based sources.
- **Lighter and more compact equipment:** optical sources, detectors and antennas are lighter and smaller compared to RF components, both on space and ground segments.
- **Lower power consumption:** FSOC consumes less power than RF because it uses optical coherent modulation with a narrower beam, which requires less power to achieve the same signal strength as RF.
- **Cost-effective:** considering the previous points, FSOC is cost-effective compared to RF communication. It leverages existing components used for fixed ground data transport through optical fibers at the same wavelength of 1550 nm.

Overall, the advantages of FSOC make it an attractive option for satellite communications, where high bandwidth, secure communication, low interference, light and compact equipment, low power consumption, and cost-effectiveness are essential.

However, this technology faces many challenges related to the effects of the atmosphere on the propagation of light signals.

Cloud cover is a major showstopper. Although some high-altitude cirrus clouds are transparent, most clouds present an extremely high attenuation (more than 100 dB) and block any optical link.

Atmospheric turbulence is another challenge. It causes random phase and amplitude fluctuations in the optical signal, leading to a degradation or a loss of data, which can impact the system's performance.

Atmospheric absorption caused by various aerosols and gases (e.g., carbon dioxide, water vapor, dusts, or ozone) also affects the propagation of light by reducing the signal strength and limiting the transmission distance.

Finally, **local weather conditions**, such as fog, rain, or snow, are also likely to block the optical link or degrade the link budget.

These limitations are unavoidable but various approaches, such as adaptive optics or error-correcting codes, can improve the system's performance and mitigate the impact of atmospheric perturbations. These techniques aim to ensure reliable and efficient data transmission between the ground and the satellite. Achieving a high availability above 99.9% required a large site diversity. Compared to RF, FSOC requires more site diversity and therefore more optical ground stations (OGS) per satellite to ensure the continuity of service. But for a given data transfer capacity, each OGS has a lower cost and is easier to deploy than an equivalent RF antenna.

Key parameters for FSOC

The monitoring of the **cloud-cover** and **atmospheric turbulence** over several months provides particularly useful information for selecting **site location and diversity** of OGS and their design. Moreover, the choice of mitigation technologies (e.g., adaptive optics) is also based on the expected distortions to compensate. Then, once the OGS is under operation, the monitoring of turbulence parameters and their predictions is still helpful for data routing and network operation.

The CCSDS Optical Communication workgroup¹ has listed key turbulence parameters. However, the list grows along time, the following sections introduce the major ones to characterize the atmosphere for FSOC applications.

Cloud cover

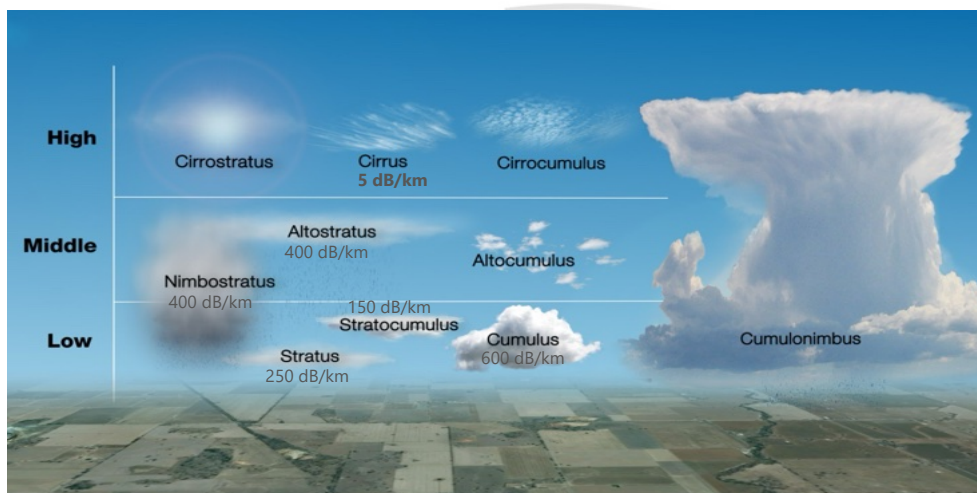


Figure 1 Attenuation due to clouds depends on their classification.

¹ <https://public.ccsds.org/publications/MagentaBooks.aspx>

Depending on their classification, clouds attenuate or even completely block the optical signal. For example, cirrus reduce the link budget by a few dB (from 3 to 7 dB) and are not showstoppers for optical communication. But most clouds generate an attenuation of hundreds of dB, which systematically block the communication. Nevertheless, the cloud cover can obscure only a part of the sky, hence the notion of fractional cloud cover.

The parameters characterizing the cloud cover are the **fractional cloud cover** (percentage of the sky on a given location that is block by clouds), the **optical density** (in percentage or density) and the **attenuation** (in dB).

Turbulence

Fried parameter r_0

The r_0 **Fried parameter** is the characteristic spatial dimension of turbulence. It represents the diameter over which the wavefront remains undistorted. The Fried parameter is a key measure of the strength of the turbulence integrated over the whole airmass between the ground and the top of the atmosphere. A large r_0 value indicates low atmospheric turbulence, resulting in a more stable and clearer optical signal.

The r_0 value depends on the temperature and the pressure of the atmosphere, the wind speed and direction and the distribution of turbulence along the atmosphere height. It is also proportional to the wavelength of the optical signal. In other words, a larger wavelength means a larger r_0 value with the same other conditions. Its values lie from a few to several dozens of centimeters, with a typical 4 cm in mild low altitude areas.

Isoplanatic angle θ_0

The **isoplanatic angle** is the characteristic angular dimension of turbulence. It refers to the maximum angle over which the wavefront remains unperturbed over the entire distance between the transmitter and receiver.

The isoplanatic angle depends on the atmospheric conditions, the distance between the transmitter and receiver, and is inversely proportional to the wavelength of the optical signal. Its values are usually comprised within ten arcsec.

Coherence time τ_0

The **coherence time** is the characteristic time of turbulence, it refers to the duration over which the received optical signal maintains a coherent phase relationship with the transmitted signal. Random fluctuations in the optical signal imply signal distortion, including scintillation and fading. These fluctuations vary rapidly, making it challenging to maintain an accurate mitigation. The τ_0 value is important as it determines the maximum time response of the mitigation technology to compensate the distortion of the signal.

The coherence time depends on the atmospheric conditions, the distance between the transmitter and receiver, and is inversely proportional to the wavelength of the signal. Its values are typically of a few milliseconds.

Scintillation

Scintillation represents the random variations in the intensity of the optical signal as it propagates through the atmosphere. These intensity fluctuations cause the signal to fade, flicker, or twinkle, similarly to how stars appear to twinkle in the night sky. This flickering can be seen on a telescope entry pupil.

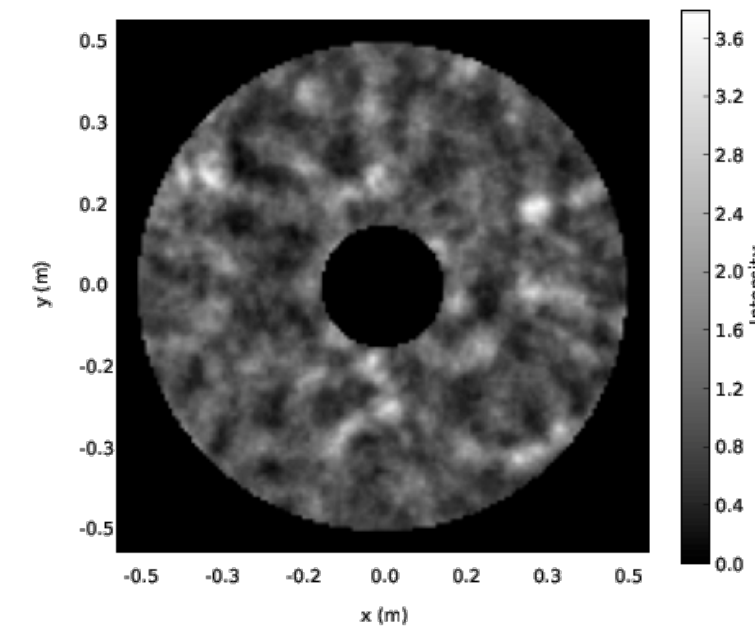


Figure 2 Scintillation is related to the fluctuation of intensity observed on the aperture of a telescope (courtesy of James Osborn)

Scintillation depends on atmospheric conditions, the distance between the transmitter and receiver, and is proportional to the wavelength of the signal and inversely proportional to the size of the telescope.

Various parameters characterize the scintillation: the scintillation index, the rytov variance and the power spectrum density.

The **scintillation index** is a measure of the intensity fluctuations in the received signal. It equals the standard deviation of the signal intensity divided by its average value. A higher scintillation index indicates more severe scintillation effects. It depends on the receiver design and its aperture.

The **Rytov variance** is the average of the squared difference between the refractive index structure function and its value at the origin, over the entire optical path.

The **power spectrum density** is a measure of the distribution of scintillation over different frequencies. It identifies the dominant spatial scales of the turbulence and to assess the performance of adaptive optics techniques.

Refractive index structure parameter C_n^2

The **refractive index structure parameter** C_n^2 is the distribution of the turbulence strength along the altitude. The optical refractive index of air varies with temperature, pressure, and humidity fluctuations, causing light to deflect as it propagates through the atmosphere. The C_n^2 characterizes these fluctuations and their distribution over the airmass. The Hufnagel-Valley model provides a typical distribution of turbulence over the altitude.

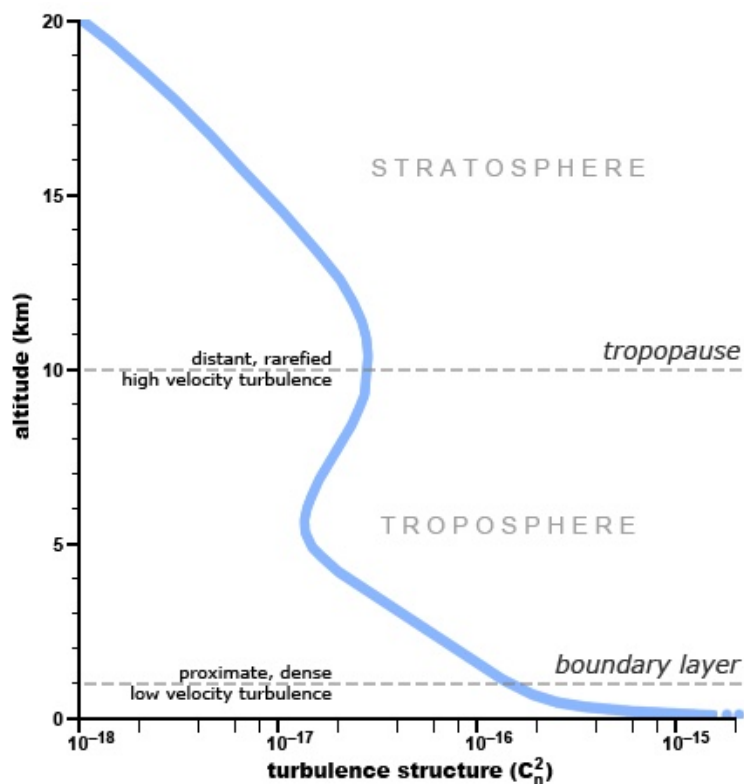


Figure 3 A typical C_n^2 profile presents a peak at the tropopause and a strong turbulence in the ground layer.

The access to the C_n^2 profile allows a fine analysis of the turbulence distribution, and the integration of C_n^2 along the altitude provides r_0 , θ_0 and τ_0 . But a turbulence profile is more complicated to measure and is not a requirement *per se*.

Aerosols

Aerosols scatter and absorb light, causing signal attenuation and degradation. The main aerosols impacting at 1550 nm are:

- carbon particles and residues of combustion due to human activities (transportation, industry, and heating).

- organic carbon particles.
- mineral dust particles (e.g., dust from Sahara in Europe).
- sea salt particles on coastal areas.
- smoke particles from wildfires or agricultural burning.

Attenuation from aerosols at 1550 nm lies from 0.1 dB/km to several dB/km, depending on the aerosol type and environmental factors. Wildfires or volcanic eruption can generate higher attenuations.

Different metrics characterize the aerosols such as the **atmospheric optical thickness** and the **angstrom coefficient**. The latter is inversely proportional to the distribution of particle size.

Water vapor

Water vapor in the atmosphere significantly attenuates light signal due to its absorption properties, which depends strongly on the wavelength.

A typical relative humidity of 50% induces a signal loss of approximately 0.25 dB/km at 1550 nm. Tropical regions with high humidity observe losses ranging from several dB/km to tens of dB/km at the same wavelength. The wavelength range around 1550 nm presents a peak of transmission, surrounded by high absorption bands. The precipitable water vapor (PWV) characterizes the water vapor in a vertical column in the atmosphere. Specifically, it is the equivalent amount of liquid water produced if all the water vapor in the column were to condense and fall as precipitation. The PWV column is provided in millimeters or centimeters.

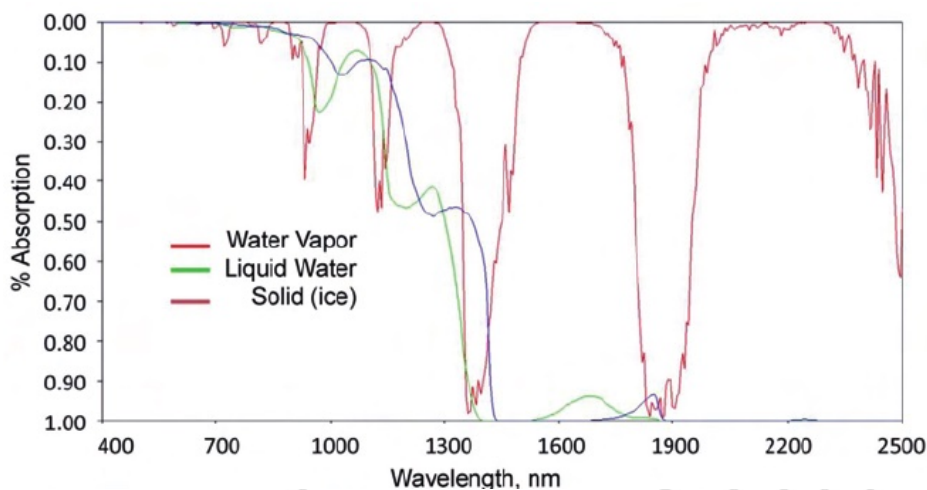


Figure 4 The absorption caused by water depends on the wavelength and the state of matter.

Overview of the instrumental solutions of Miratlas

Miratlas' Sky Monitor covers extensively all the parameters required for performances management and system dimensioning for FSOC. The following sections presents the instruments and their operation.

The Sky Monitor

The Sky Monitor is Miratlas' main instrument, it consists in a control unit embedding part of the instrumentation as well as the processing board. The main unit also includes a giga Ethernet (GigE) switch with power over Ethernet (PoE) to connect other subsystems.

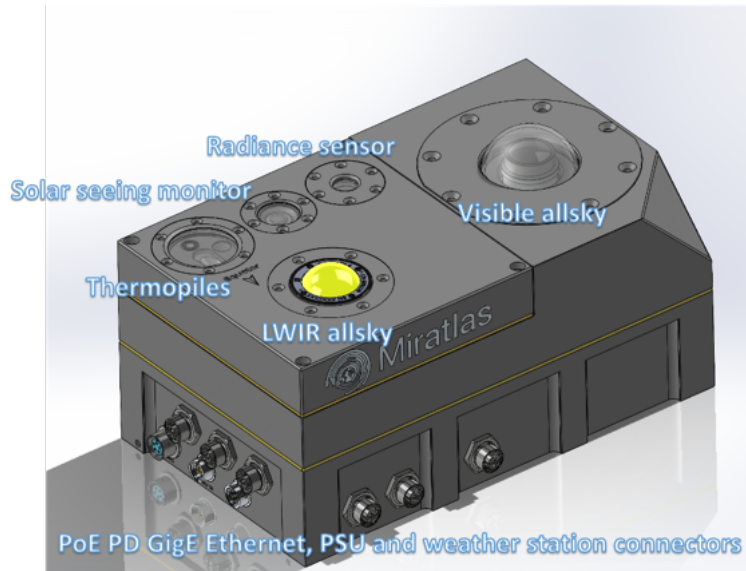


Figure 5 The Sky Monitor v4 control unit integrates visible and radiometric LWIR all sky cameras.

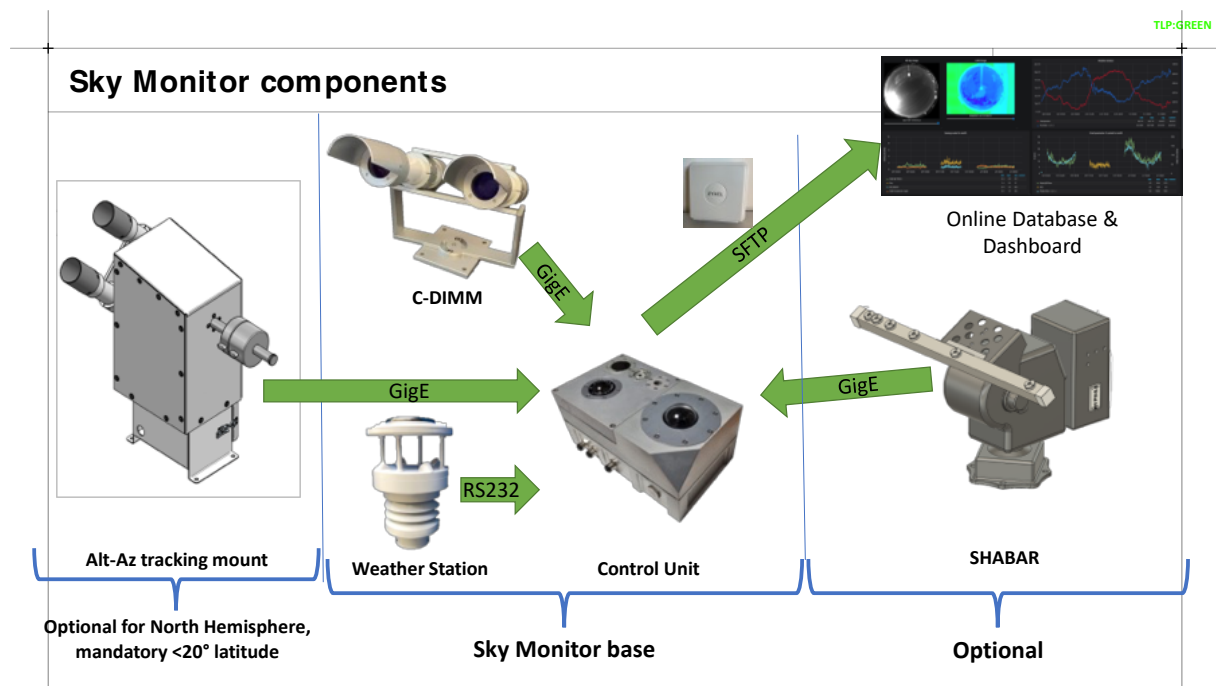


Figure 6 The control unit and the other instruments deliver all the parameters needed to monitor turbulence.

Weather parameters

Acquired data: **temperature, pressure, humidity, wind and rain**

A calibrated weather station measures local weather parameters every minute with. A heatshield protects pressure, temperature, and humidity sensors, while wind is measured with 2D ultrasonic anemometers and rain rate is measured with a piezoelectric sensor.

Turbulence

Daytime measurement using solar scintillation

Acquired data: r_0

The Sky Monitor estimates the Fried parameter r_0 during daytime using solar scintillation. E. Seykora² and J. Beckers³ introduced the concept in the nineties. A photometer measures the intensity fluctuations of the sun light disturbed by atmospheric turbulence. Assuming the turbulence is homogeneous and isotropic along the propagation path, a relation between the refractive index structure parameter C_n^2 , the wavelength λ and the scintillation index σ^2 at the ground level is provided as follows:

$$C_n^2 = 2.91e^{-17} / (\lambda^2 \sigma^2)$$

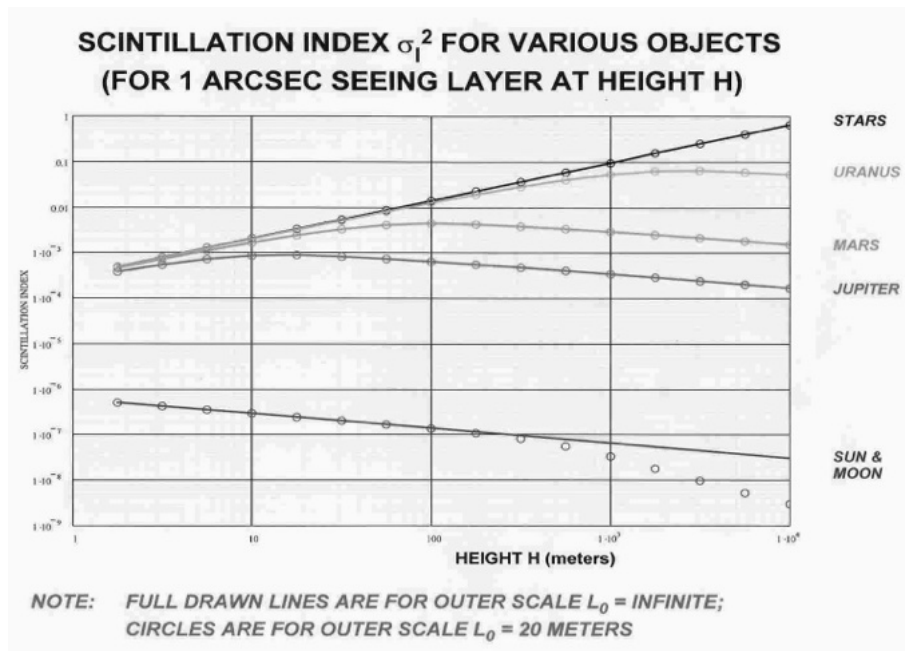


Figure 7 Scintillation index depends on the altitude in the atmosphere.

The refractive index structure parameter C_n^2 is related to the Fried parameter r_0 :

$$r_0 = (0.423 k^2 L_0 C_n^2)^{-3/5}$$

² Seykora, E. J. (1993). Solar scintillation and the monitoring of solar seeing. *Solar Physics*, 145, 389-397.

³ Beckers, J. M. (1993). On the relation between scintillation and seeing observations of extended objects. *Solar Physics*, 145, 399-402.

Where k is the wave number ($k = 2\pi/\lambda$) and L_0 the outer scale of the turbulence.

The scintillation index depends on the size of the observed object and the altitude at which measurement is performed. The larger the object the smaller the scintillation. Low altitude turbulence contribution is stronger than high altitude jet streams for extended objects (e.g., the Sun and the Moon). While for stars, the contributions are reversed because they are spatially coherent sources.

For the Sun, low altitude scintillation (flying shadows from the first meters) can be as large as 0.3 arcsec, but in most case it is about 10^{-4} to 10^{-5} . The Jetstream contribution is low and barely detectable. Therefore, the scintillometer embedded in the Sky Monitor is only sensitive to the boundary layer which is the dominant contribution during daytime.

Daytime measurement with SHABAR (optional)

Acquired data: r_0 , θ_0 , τ_0 , and C_n^2 along the altitude



Figure 8 The SHABAR is a daytime turbulence profiler mounted on a tracking mount.

The SHADow BAnd Ranger (SHABAR) is a daytime turbulence profiler. Originally developed by astronomers in the nineties, Miratlas has commissioned an updated version of the instrument for the supporting FSOC applications. The instrument is composed of an array of six photodiodes unevenly aligned and facing the Sun. The line of photometers is fixed on a motorized mount to track the Sun position along the day. Each photometer measures the sun light scintillation, as the Sun is an extended light source, the degree of correlation between the different channels depends on their separation distance. The closer are the photodiodes, the higher the correlation.

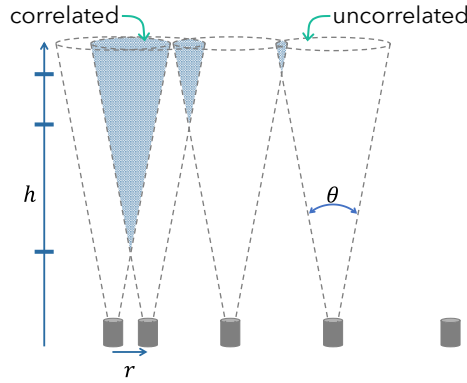


Figure 9 The degree of correlation between two photodiodes observing the Sun depends on their separation distance.

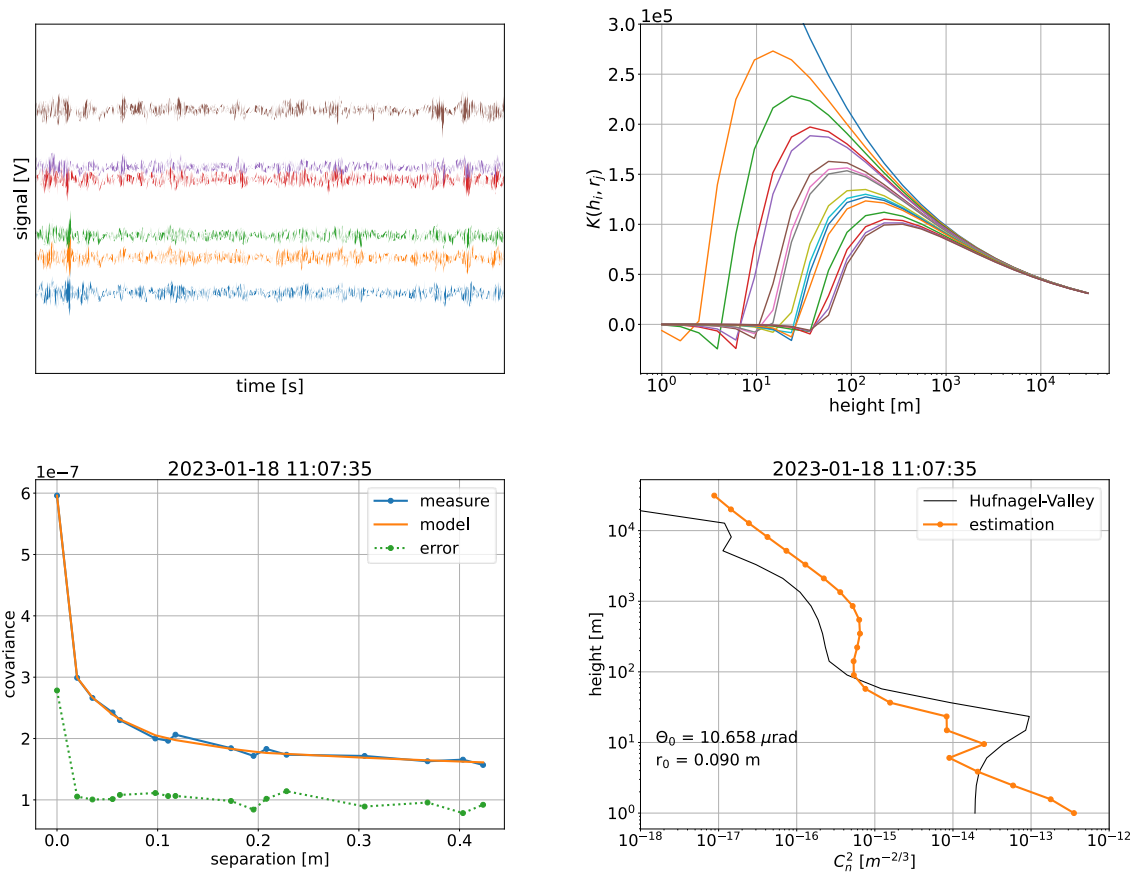


Figure 10 (top left) Raw signals acquired along time show some bursts due to turbulence. (top right) The kernel function K depends on the altitude and the separation distance. (bottom left) The covariance model is adjusted to minimize the distance to the measured covariance values. (bottom right) The C_n^2 values estimated from the modeled covariance show a typical turbulence profile. The Hufnagel-Valley profile is shown as a matter of illustration, not for formal comparison.

The measurements are processed to evaluate the covariance between each pair of channels. This measured covariance is then approached a modeled covariance to finally get an estimation of the refractive index structure constant along the altitude $C_n^2(h)$.

Nighttime measurement with C-DIMM

Acquired data: r_0 , θ_0 , τ_0

The Differential Image Motion Monitor (DIMM) is a nighttime turbulence monitor using scintillation of stars. Astronomers⁴ widely use this technique and Miratlas as commissioned a compact version of the instrument for FSO applications that is called Compact-DIMM (C-DIMM).



Figure 11 The C-DIMM can be mounted on an astronomical mount (shown here without its enclosure) to track stars during the night.

The DIMM technique involves two apertures, on one or two telescopes, separated by a known distance. The two apertures observe simultaneously the same point source, a star in our case. An image of the star is acquired on both apertures with cameras. Because of the turbulent atmosphere, the two images formed by the apertures are not identical. The differential image motion is due to the tilt order of the atmospheric turbulence and is proportional to the **Fried parameter** r_0 . The variance of the differential image motion along the longitudinal (σ_L^2) and the transverse (σ_T^2) axes is:

$$\sigma_L^2 = 2\lambda^2 r_0^{-5/3} (0.179D^{-1/3} - 0.097d^{-1/3})$$

$$\sigma_T^2 = 2\lambda^2 r_0^{-5/3} (0.179D^{-1/3} - 0.145d^{-1/3})$$

where D is the diameter of the apertures and d their separation distance. The **Fried parameter** r_0 is estimated from σ_L^2 and σ_T^2 . The **coherence time** τ_0 is also estimated from this differential motion, while the **isoplanatic angle** θ_0 is derived from the scintillation of the star under observation.

⁴ Sarazin, M., & Roddier, F. (1990). The ESO differential image motion monitor. *Astronomy and Astrophysics (ISSN 0004-6361)*, vol. 227, no. 1, Jan. 1990, p. 294-300., 227, 294-300.

Usually, the DIMM is based on a 250-300 mm aperture telescope with two sub-apertures fitted with prisms to provide two images of the same star. The C-DIMM of Miratlas is much more compact and weatherproof. It uses two optical tubes of 50 mm aperture, separated by 200 mm, and two synchronized cameras. This configuration is like a C11 telescope (280 mm diameter) with two apertures that is usually used by astronomers for DIMM instrumentation. The C-DIMM has been designed to work with Polaris star in northern hemisphere without any tracking. But it can also be fitted on an automated tracking mount for tracking any other sufficiently bright star, suitable for operations all over the world and for complete sky survey.

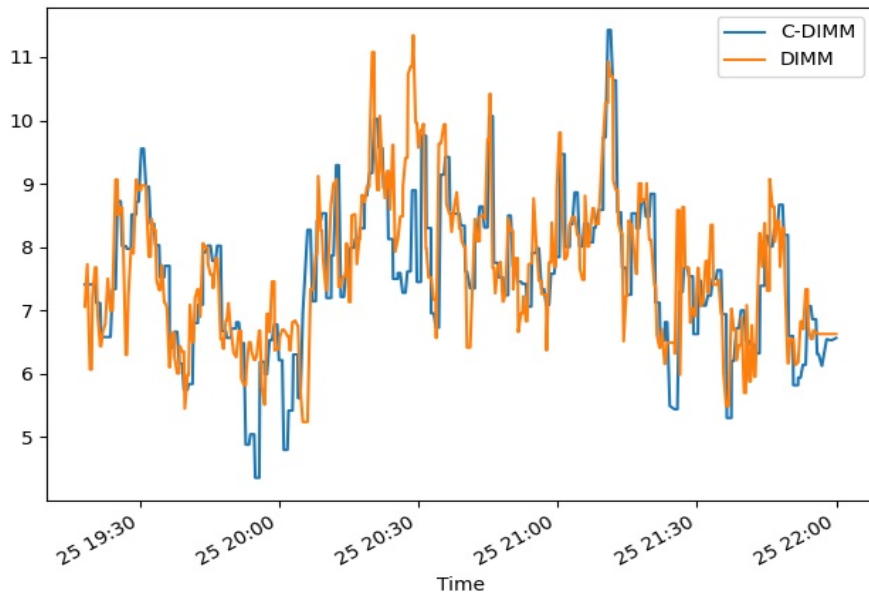


Figure 12 The angles of arrival (in degree) measured by the C-DIMM and a standard DIMM on a C11 telescope show a good agreement over time, validation campaign made in 2019.

Irradiance

Irradiance measurement

Acquired data: **visible irradiance**

A large dynamic photodiode embedded in the Sky Monitor central unit gives the sky irradiance in $mag/arcsec^2$. It has a 40° field of view (FoV) to reduce the influence of local straylight. The sensor gives a rough estimation of light pollution and backscattered light in urban environment.

Radiance measurement (optional)

Acquired data: **visible** and **SWIR sky radiance**

An 80 mm telescope collects light from sky with a 10° FoV, mounted on tracking mount, it can measure sky radiance at different elevation and azimuth during day and night. It operates at

800 nm and 1550 nm with a spectral resolution of ~ 100 nm. The accessible radiance range goes down to $10^{-5} W/m^2/sr/\mu m$. This measurement is dedicated to single photon applications such as quantum key distribution, where sky radiance is an important source of noise in the signal.

Thermal infrared irradiance

Acquired data: **sky temperature** at zenith and North, **back scattered thermal radiation**

The Sky Monitor embeds two long wave infrared (LWIR) radiometric thermopiles, one facing zenith with a 10° FoV, the other facing the opposite direction of the equator at an elevation of 52° and with 40° FoV. These sensors deliver the temperature of the sky. They are used amongst other application to check if the zenith is clear or cloudy (background sky is colder than clouds), and to calculate the back scattered thermal radiation.

Aerosols

Differential absorption solar photometer (optional)

Acquired data: **angstrom coefficient**, **atmospheric optical thickness** at 465, 540 and 619 nm

The solar photometer is a rework of an existing handheld instrument qualified by the Atmospheric Optics Laboratory (Lille, France). Each device is calibrated individually at Izaña observatory (Tenerife, Spain). The photometer is mounted on a tracking mount to follow the Sun during daytime. The device provides the atmospheric optical thickness and the angstrom coefficient. The latter is inversely proportional to the distribution of the size of the particles in the atmosphere.

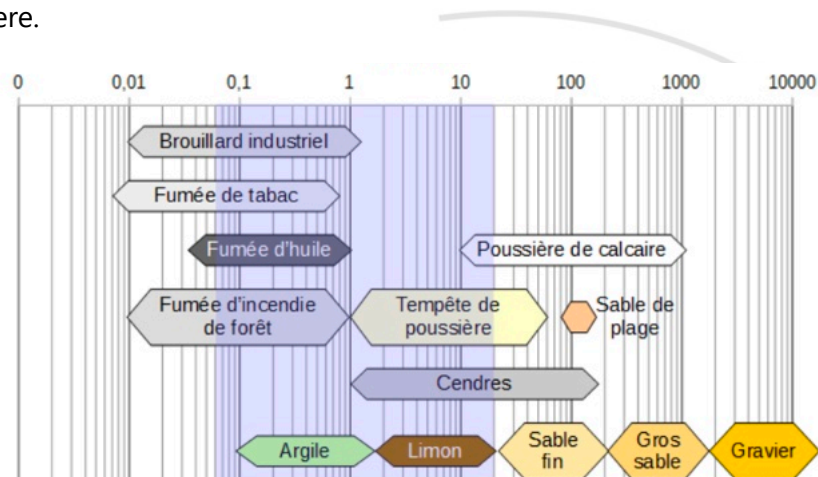


Figure 13 The solar photometer is sensitive to particles from $0.06 \mu m$ to $20 \mu m$ (fog, combustion smoke, wildfire, dust storm, ashes).

Precipitable water vapor

Acquired data: **precipitable water vapor** (PWV)

The Sky Monitor embeds a rough estimation of PWV using LWIR backscattering but this only works with sunlight.

A new PWV estimation based on GPS (global positioning system) has been commissioned. GPS signals are affected by the water vapor as it slows down their propagation. The PWV is inferred from the propagation delays measured on two frequencies L1 (1575.42 MHz) and L2 (1227.6 MHz).

Allsky cameras

Visible allsky cameras

Acquired data: monochrome visible **allsky images**, nighttime **absolute transparency map**

The Sky Monitor integrates a camera with a fisheye lens providing full sky coverage at visible wavelength. The camera has an automatic gain and exposure time ranging from a few μs by daytime, to 10 s at nighttime. It can detect stars with magnitude lower than 6 and therefore measure over 1500 stars in a single image. The images are also helpful for cloud detection during daytime. Clouds are sometimes difficult to detect on these visible images during nighttime.

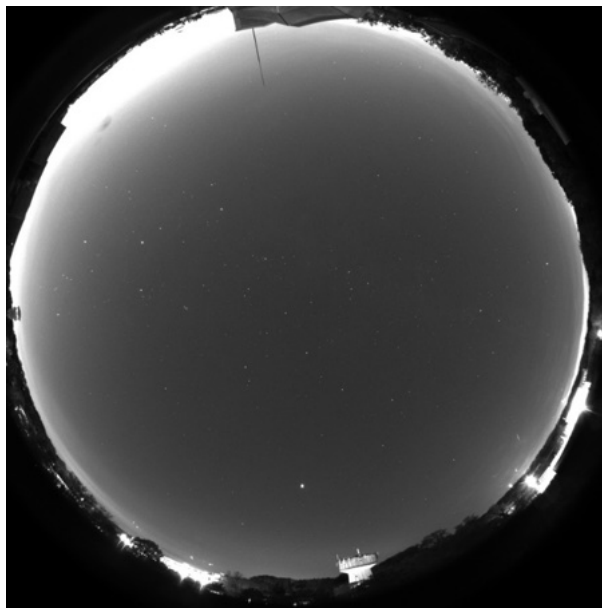


Figure 14 During nighttime, the allsky camera sees 1500+ stars and evaluate sky absolute transparency, image taken in Paris suburbs.

Images have an effective size of 2064 x 2064 pixels (4 Mpx) with a monochrome dynamic of height bits. The sensor delivers low noise images ($< 1e^-$), with low thermal noise. Hot pixels are corrected by a dark reference frame. The distortion is corrected to f -theta and an absolute transparency map is generated at nighttime using an astrometric resolution.

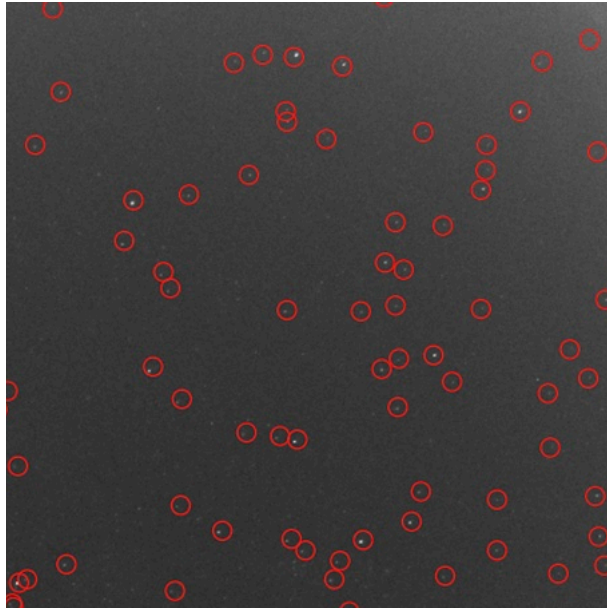


Figure 15 The astrometric resolution processed on allsky images identify the stars referenced in catalogs. Identified stars have a magnitude lower than 5.5 but fainter stars are also visible.



Figure 16 Allsky image taken during nighttime at Teide Observatory (Izaña, Spain).

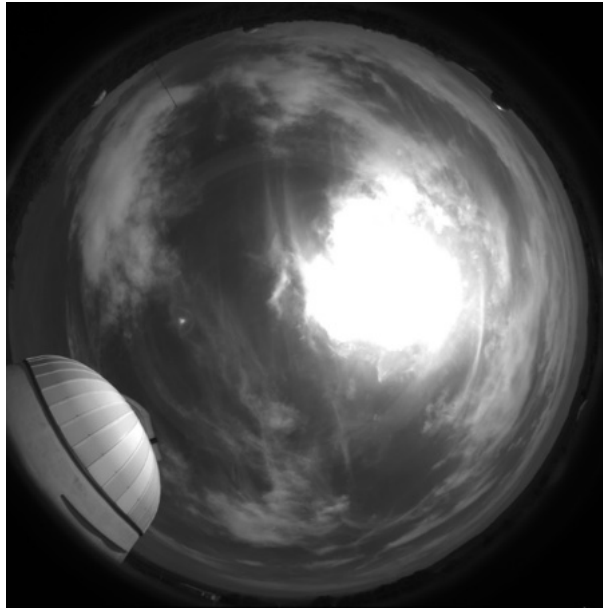


Figure 17 Clouds are detected on allsky images during daytime. The image has been taken at the Haute Provence Observatory (France) and shows cirrus clouds, as well as contrails.

LWIR thermal allsky cameras (optional)

Acquired data: **allsky calibrated temperature image**

An optional allsky thermal camera with radiometric calibration delivers an f -theta corrected image of the sky temperature. The first version of the instrument used an independent camera and a large metallic mirror (gold or aluminium coating).



Figure 18 First version of the LWIR allsky camera and its gold coated mirror. The C-DIMM is also visible at the foreground of the picture. Image taken at the Teide Observatory (Izaña, Spain).

An updated version using a fisheye lens has been commissioned and is directly embed in the Sky Monitor main unit. The thermal allsky camera detects clouds during both daytime and

nighttime. It can also detect contrails which take part in the generation of cirrus clouds under some conditions.

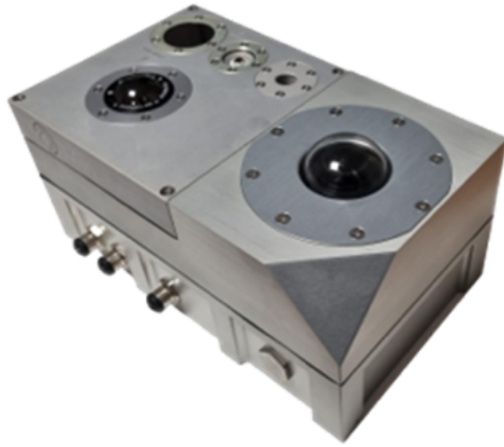


Figure 19 A new LWIR allsky camera is optionally embedded directly in the Sky Monitor central unit.

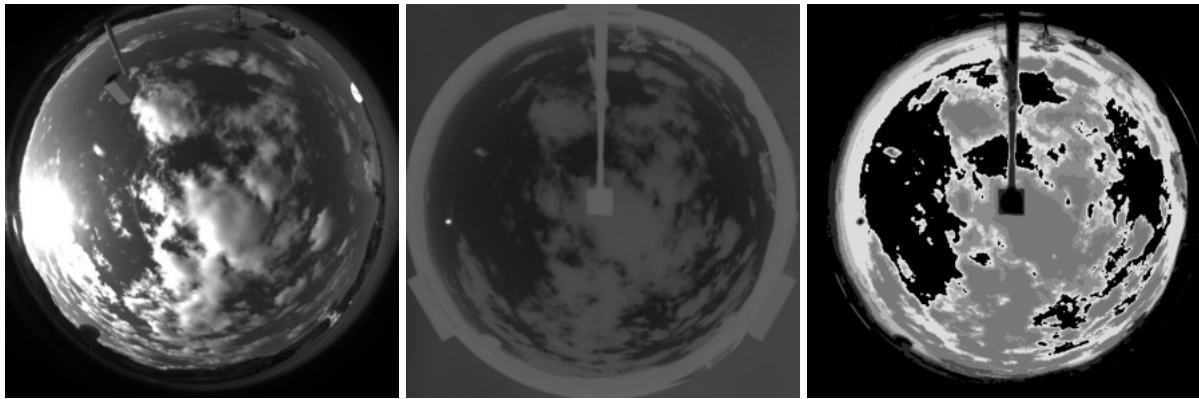


Figure 20 Visible (left) and LWIR (middle and right) images taken simultaneously illustrate the ability to detect clouds on both images. The image on the right is processed to sort out clouds by their altitude. Images taken at Canberra Deep Space Communication Complex (Canberra, Australia)

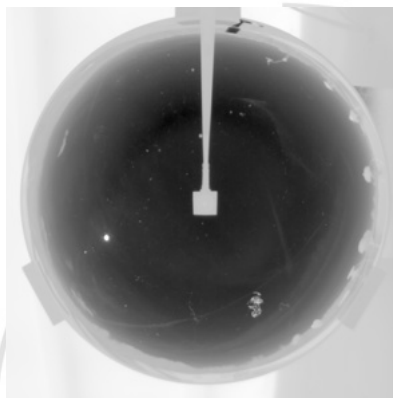


Figure 21 Thermal allsky images can also detect the formation of contrails.